Evaluation of the reliability of high concentrator GaAs solar cells by means of temperature accelerated aging tests

N. Núñez[1,2]*, J. R. González[1], M. Vázquez[1,2], C. Algora[1] and P. Espinet[1]

[1] Instituto de Energía Solar-Universidad Politécnica de Madrid, Ciudad Universitaria s/n, 28040 Madrid, Spain
[2] EUIT Telecomunicación-Universidad Politécnica de Madrid, Carretera de Valencia Km 7, 28031 Madrid, Spain

ABSTRACT

Evaluating the reliability, warranty period, and power degradation of high concentration solar cells is crucial to introducing this new technology to the market. The reliability of high concentration GaAs solar cells, as measured in temperature accelerated life tests, is described in this paper. GaAs cells were tested under high thermal accelerated conditions that emulated operation under 700 or 1050 suns over a period exceeding 10 000 h. Progressive power degradation was observed, although no catastrophic failures occurred. An Arrhenius activation energy of 1.02 eV was determined from these tests. The solar cell reliability [R(t)] under working conditions of 65°C was evaluated for different failure limits (1–10% power loss). From this reliability function, the mean time to failure and the warranty time were evaluated. Solar cell temperature appeared to be the primary determinant of reliability and warranty period, with concentration being the secondary determinant. A 30-year warranty for these 1 mm^2-sized GaAs cells (manufactured according to a light emitting diode-like approach) may be offered for both cell concentrations (700 and 1050 suns) if the solar cell is operated at a working temperature of 65°C.

KEYWORDS

concentrator photovoltaic; CPV solar cells; reliability; warranty

***Correspondence**

Neftalí Núñez, Electrónica-Física, EUIT Telecomunicación-UPM, Carretera de Valencia Km 7, 28031 Madrid, Spain.
E-mail: neftali.nunez@upm.es

1. INTRODUCTION

Significant advances have been made in the field of III–V high-concentrator multijunction solar cells (MJSCs), achieving peak efficiencies of 32.6% at 1000 suns for a dual-junction solar cell [1] and 43.5% at 418 suns for a triple junction solar cell [2].

Concentrator photovoltaic (CPV) systems are among the devices under development that show the most promise for reducing electricity costs. A key concern is preserving the initial quality of CPV systems during long operational periods (reliability) [3]. Aware of this problem, the CPV community has developed a new standard (IEC-62108:2007) for qualifying CPV modules and assemblies [4].

The current industrial landscape includes companies that manufacture both solar cells and systems, as well as companies that manufacture systems using cells purchased from others (hereinafter, integrators). No generally-accepted standards exist for qualification of bare solar cells, even though the WG7 TC82 (responsible for drawing up the IEC-62108:2007 standard) is moving forward to overcome this situation. Assessments of the reliability and degradation of concentrator solar cells remain scarce [5].

If CPV systems are to be competitive with conventional silicon flat module technologies, they must present similar warranties (i.e., 25–30 years). With the IEC-62108:2007 qualification standard in place, and with the installation of almost 3 MW deployed in ISFOC [6] (a powerful benchmark for CPV systems), efforts must be applied toward assessing the reliability of concentrator III–V solar cells. Accelerated tests and reliability statistical methods must be applied to III–V concentrator MJSCs to determine the main reliability functions.

The III–V concentrator solar cells display a technology and properties similar to those of some light emitting diodes (LEDs). A prediction of the mean time to failure (MTTF) of at least 10^5 h (equivalent to 34 years, assuming an average of 8 h of operation per day) for concentrator

solar cells was made by Vazquez *et al.*[7]. MTTF value predictions for GaAs concentrator solar cells have later been evaluated by means of step–stress accelerated aging tests, from which a maximum likelihood estimation of the MTTF was calculated to be 8.64×10^6 h [8].

With the aim of precisely determining the main reliability functions, this paper presents a set of temperature accelerated aging tests conducted for GaAs single junction solar cells. These tests measured the activation energy associated with the degradation mechanism, as well as the acceleration factor, the MTTF, and the reliability function, among other performance measures. After calibration of all procedures, equipment, and models for the concentrator GaAs single junction solar cells, the reliability of the MJSCs will be tackled in a straightforward way. It should be noted that failure analysis was not the aim of this work.

2. TEMPERATURE ACCELERATED AGING TESTS

2.1. Procedure

The stress parameter most frequently used to accelerate aging in electronic devices is temperature. Most physical and chemical processes involved in device degradation follow Arrhenius law [9,10]. The accelerated aging time, therefore, depends exponentially on the temperature. Consequently, the figures of merit used to describe the reliability of semiconductor devices depend on temperature.

A temperature stress accelerated aging test involves introducing devices into a climatic chamber, and adjusting the nominal working conditions, except for the temperature which is higher in order to accelerate the aging process. The test procedures used here to test high concentrator GaAs single-junction solar cells are described elsewhere [11]. The test conditions were similar to those used in previous tests, described in [8], with several new features:

1. The accelerated life test method used here was the accelerated life test (ALT), which yields quantitative information that is more reliable than that gleaned from the highly accelerated life test (HALT) method [8]. ALT tests are designed to estimate product reliability. In contrast, the primary purpose of HALT tests is not to measure but to improve reliability. HALT tests are used in the early design and development phases to reveal potential failure modes. These two types of tests are described in detail in [12].
2. A new data acquisition system was designed and built. Its full description can be found elsewhere [13].
3. A new method for encapsulating solar cells using direct bonded copper substrates (DBC) was implemented. This encapsulation technique provided good thermal management and minimized the risks associated with failure of elements not in the solar cells.
4. Three temperatures and two concentration ratios were applied. All tests were conducted over more than 10 000 accumulated hours.

The emulation of concentrator solar cell working conditions in climatic chambers presents several technological challenges. The key concern is identifying suitable ways to emulate constant illumination levels in the range of 1 000 suns. For the cells tested here, the working conditions were emulated under a forward bias at a current density equal to that which would have been photogenerated by the cell at the nominal concentration. This approach emulated the electrical stresses in the semiconductor material experienced by a solar cell operating under realistic electric conditions, and the thermal stresses. However, this method did not consider the stresses attributable to high irradiance levels in the optical concentrator. Further testing should be performed, and the relevant techniques are currently under development [5]. Such additional tests will not be discussed here.

The reliability tests were conducted at three temperatures (130°C, 150°C, and 170°C) at two emulated concentrations, 700 and 1050 suns. Cells without a forward bias (i.e., storage conditions) were also included for reference purposes.

A method for predicting the illumination *I–V* curve from the dark *I–V* curve at the working concentration was first presented in [14] and later applied to reliability tests in [8]. Using this method, the experimental data recorded for the dark *I–V* curve of the cells could be used to reproduce the illumination curve by knowing the short-circuit current (which was measured under illumination prior to the aging test) and the series resistance (which was obtained by fitting the dark *I–V* curve to a two-diode model). The illumination curve obtained from this method could be used to calculate the maximum power. The evolution of the solar cells throughout the aging process was followed by recording the ratio of the maximum power to the initial power ($P_t/P_{t=0}$).

2.2. Experimental

The GaAs high-concentrator solar cells used in this work were manufactured on semiconductor structures grown in a metal-organic vapor phase epitaxy (MOVPE). Devices were fully processed in the Instituto de Energía Solar using optoelectronic techniques [15] to get small area solar cells. A description of the manufacturing process can be found elsewhere [16].

Tests were conducted using 1 mm^2 high-concentrator GaAs single-junction solar cells. In previous work [8], this type of cell failed at the unprotected perimeter. For this reason, the cells tested here were covered (protected) with a silicone material commonly utilized in photovoltaic applications. Covering with a silicone layer emulated the real conditions of a cell mounted inside the secondary optics of a concentrator. Finally, the DBC substrates were attached to an aluminum box using a thermally conductive

adhesive. Figure 1 shows the encapsulated solar cells inside a climatic chamber.

Each encapsulation setup, as shown in Figure 1, housed 18 cells. As mentioned in the previous section, the DBC substrate material used to assemble the cells was selected for its good thermal conductivity and resistance to the high temperatures at which these tests were conducted. The measurement method setup used to emulate the working conditions and the method used to determine the solar cell junction temperature during tests are described in detail in [13].

Table I shows the testing temperatures and the total test duration, together with the number of cells tested at each concentration for each temperature (for the sake of simplicity, 0X indicates the emulated dark condition, i.e., no illumination, and no bias was applied). It should be noted that only the periods during which the cells were biased were considered to be part of the test duration. The results of the lowest temperature test (the evolution of the solar cell power loss at 130°C) were used to determine both the temperatures (150°C and 170°C) and the time between measurements for the other test conditions. Accordingly, the suitable period was determined experimentally, 18 h for the 130°C test and 3 h for the 170°C test. Additional details are provided in [13].

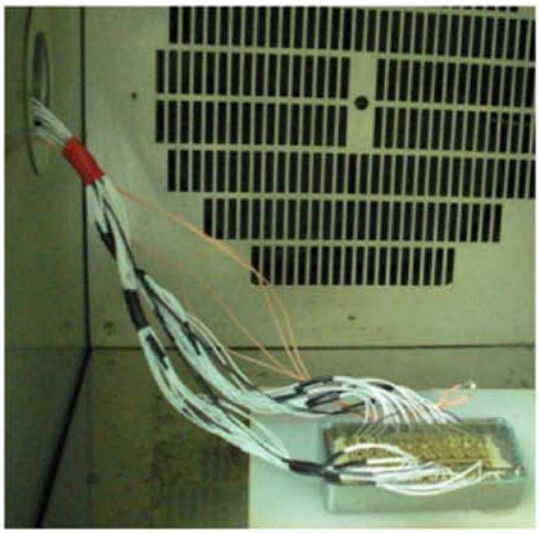

Figure 1. Solar cells encapsulated within a direct bonded copper substrate and covered with silicone inside an aluminum box in the climatic chamber.

Table I. Temperature of each test, duration, and number of cells tested at each emulated concentration.

		Number of cells at		
T (°C)	Duration (h)	0X	700X	1050X
130	4232	4	14	—
150	5612	3	10	5
170	1026	6(*)	12	—

The symbol (*) means that three of six cells were used for reference purposes and were only measured at the beginning and end of the test. No performance differences were found between the periodically measured cells and the reference purposes cells.

3. RESULTS

Figure 2 shows the dark *I–V* evolution of a solar cell. This curve is representative of the degradation results in the solar cell tests.

A key consideration in reliability measurements is the definition of suitable failure criteria. Two possibilities may be proposed:

- Catastrophic failure: the sudden breakdown of a solar cell, which results in an abrupt loss of power.
- Degradation failure: we consider as a failure for the CPV system when its power decreases more than 20% compared with the initial power. This power loss is typical of silicon flat modules [17]. Accordingly, we have defined a 2.5% solar cell power loss as the failure limit. At this limit, the other elements of the CPV system could contribute to the remaining power loss up to a 20% failure limit for the whole system. This failure criterion for concentrator cells is considered to be conservative.

The experimental results show the following:

- That no catastrophic failures were found in the solar cells tested at the three temperatures and at the two emulated concentrations. In other words, only degradation failure occurred.
- There is not any relationship between the initial solar cell power and the degradation value observed.

The results of the average relative power loss in each test are presented in Table II.

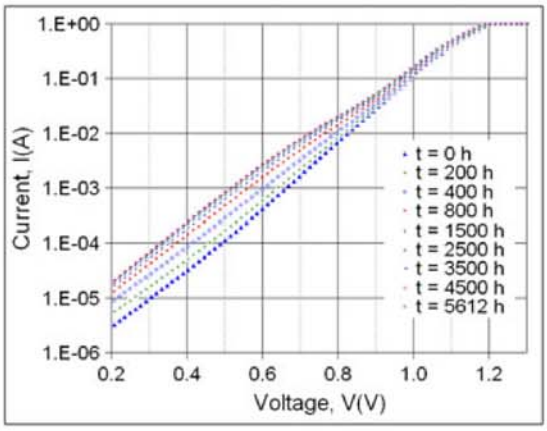

Figure 2. Dark *I–V* curves for a representative solar cell tested at 150°C and a current injection equivalent to 1050X.

Table II. Average relative power loss at the end of each test.

		Average relative power loss (%)		
T (°C)	Duration (h)	0X	700X	1050X
130	4232	0.24	1.69	—
150	5612	0.68	2.78	5.87
170	1026	0.55	2.57	—

Figure 3 shows the average relative power evolution over time for the 170°C test and no current injection (0X). A low average degradation, which nearly followed a straight line, was observed. Cells tested without current injection showed negligible variations in their dark *I–V* curves during tests.

The tests in which cells were submitted to a forward bias showed three stages with different slopes in the relative power versus time plots (see the left-hand region of Figure 4), which indicated different velocities for the relative power losses. After a brief initial stage, during which degradation was negligible, the plots continued into a second stage with a power degradation velocity significantly higher than that observed in the subsequent third stage, during which the loss tended to stabilize. For the sake of simplicity in the subsequent discussion, the terms second and third stages will be used to refer to these regions of the relative power versus time plots.

In the second stage (with a high-power degradation velocity), some of the tested cells presented a significantly higher degradation, which increased the standard deviation and the relative power slope (see the right-hand region of Figure 4).

In the third stage, the relative power loss of all cells tended to stabilize. Consequently, the standard deviation showed a trend toward stabilization.

3.1. Activation energy and the acceleration factor as a function of temperature

The time acceleration factor (*AF*), between the period of accelerated tests and the correspondent period of real operation was determined as a function of temperature for a given concentration using an Arrhenius model. In such a model, the velocity of a chemical reaction depends on the temperature according to an exponential law. Following the Arrhenius life-stress model, device lifetime can be expressed as

$$L(T) = Ae^{\frac{E_A}{kT}} \tag{1}$$

where $L(T)$ indicates a quantifiable performance measurement and T is the temperature representing the stress level of a test. Here, $L(T)$ is the particular time ($t_i(T)$) at which the average relative power has a given value (P_i/P_0). A is an Arrhenius parameter that depends on the selected L value and on the device, and is not necessary for obtaining AF. k is Boltzmann's constant, and E_A is the activation energy of the defects to be determined in the test.

To determine whether these tests followed an Arrhenius model [9,10], four equidistant values of the relative power loss at the three temperatures were considered. The maximum average relative power loss common to the three different tests temperatures at 700X was 1.69% (achieved at 700X for $T = 130$°C, see Table II). $L(T)$ in Equation (1), is the particular time ($t_i(T)$) at which the average relative power has a given value (P_i/P_0) being this value lower than 1.69%.

Accordingly, power loss values of 1.6%, 1.2%, 0.8%, and 0.4% were considered. The time values ($t_i(T)$) at which these relative power losses increased by 0.4% are represented for the three tested temperatures in an Arrhenius plot shown in Figure 5. The three points corresponding to the same average power loss for the various temperatures could be fit to straight lines, indicating that the tests followed an Arrhenius model. The activation energy (E_A) was determined from the slope (E_A) of these plots $[\ln(t_i(T)) = E_A \cdot (1/kT) + \ln(A)]$, yielding an activation energy of 1.02±0.04 eV. To the best of our knowledge, this is the first time the activation energy associated with a degradation mechanism has been calculated for III–V concentrator solar cells.

Once the activation energy was known, the AF of the degradation mechanism for two given temperatures could be obtained [18]:

$$AF = \frac{t_i(T_{\text{use}})}{t_i(T_{\text{acc}})} = \exp\left[\frac{E_A}{k}\left(\frac{1}{T_{\text{use}}} - \frac{1}{T_{\text{acc}}}\right)\right], \tag{2}$$

where T_{use} is the expected operation temperature and T_{acc} is the accelerated test temperature.

Differences in the final test times and P_i/P_0 at which the solar cells were temperature-stressed (see Figure 4) prompted an investigation into whether the degradation ratios of the cells, which depended on the activation energy extracted from Figure 5, were constant for average relative power losses higher than 1.69%. Figure 6 shows the relative power measured in the three temperature tests for the 700X cell over times equivalent to the 130°C test time. This required that the test times of the 150°C and 170°C tests were multiplied by the corresponding AF values for $E_A = 1.02$ eV at 130°C (i.e., 4.01 for 150°C and 14.18 for

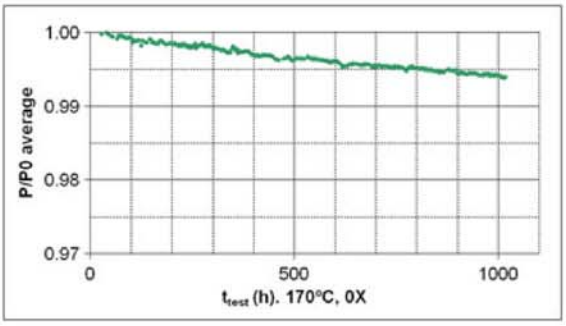

Figure 3. Average relative power evolution over time for the 170°C test, for cells without current injection (0X).

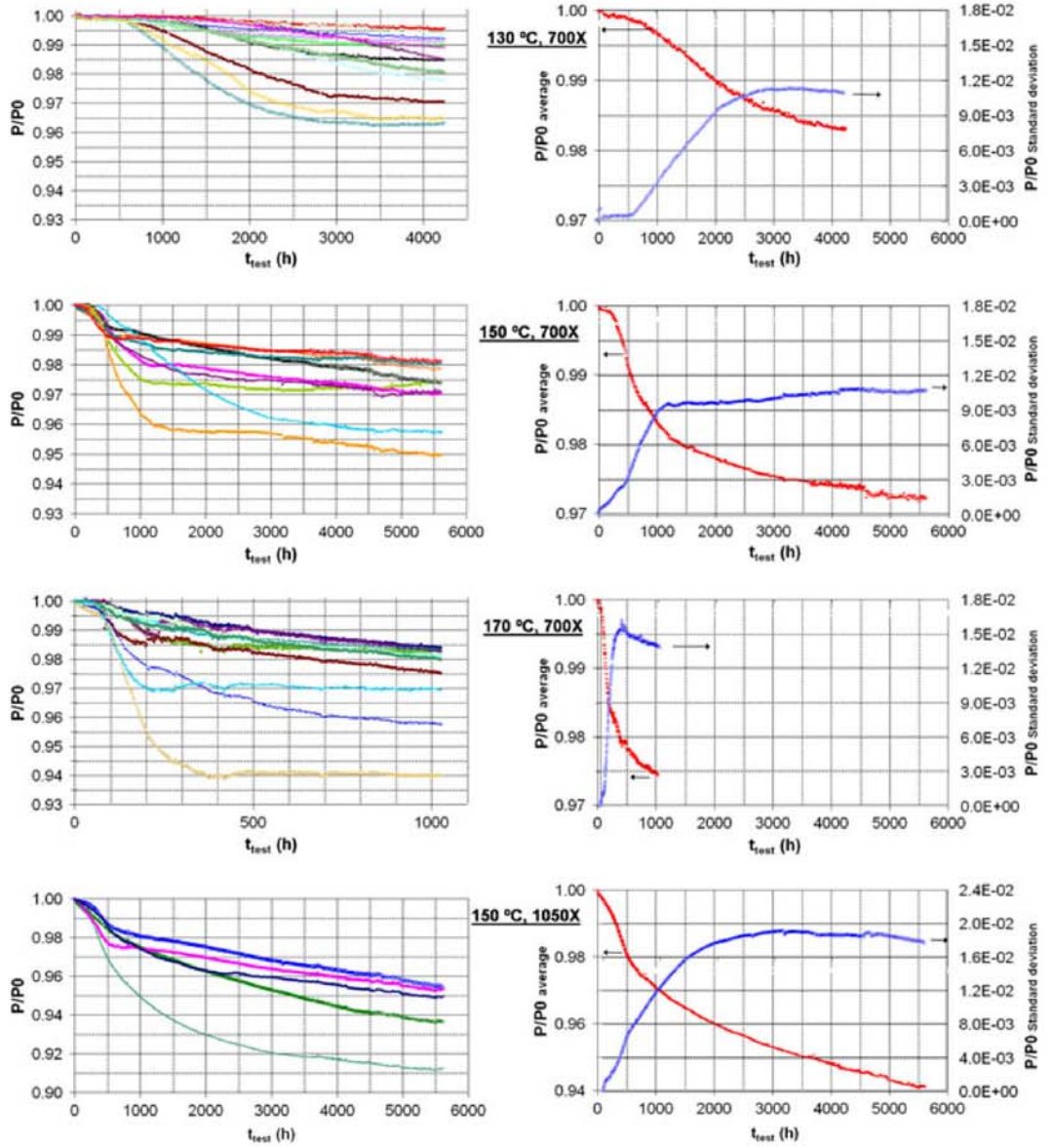

Figure 4. Sequence of plots of the relative power versus time of test for all cells tested (left), and the average relative power versus time together with the standard deviation versus time (right) for the four conditions of temperature and concentration. Note that the left-hand figures were shown with a different time scale for clarity.

170°C, obtained from Equation (2)). The good fits of the three average relative power curves over the duration of the long lifetime accelerated tests justified the use of the test results with the longest duration (5612 h for $T = 150$°C) to extrapolate the average relative power (and conversely, the power loss) of the solar cells at any temperature using the value of AF obtained from Equation (2).

Accordingly, Figures 7 and 8 show the average relative power for both the 700X and 1050X solar cells at different expected operation temperature for continuous operation. These figures show that the working temperature significantly influenced the power evolution. Thermal management, therefore, is crucial for controlling solar cell power degradation.

Assuming a typical operational temperature of 65°C for small and 1000X concentrator solar cells [19], Figures 7 and 8 show an average power reduction of 2.5% at 700X after 3.29×10^6 h of continuous operation. Similarly, the 2.5% power reduction of the 1050X cell appeared after 8.05×10^5 h continuous operation.

3.2. Influence of concentration.

The ratio between the two concentrations used for the preparation of the concentration cells tested here (700X and 1050X) was 1.5, and the ratio of the injected current strengths, therefore, was also 1.5. Figures 7 and 8 permit

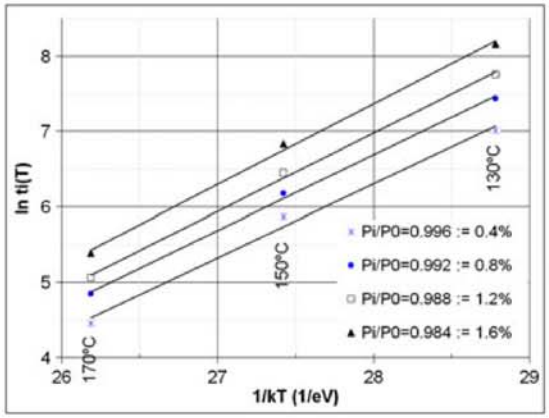

Figure 5. Arrhenius life-stress plot for four power loss values at 700X.

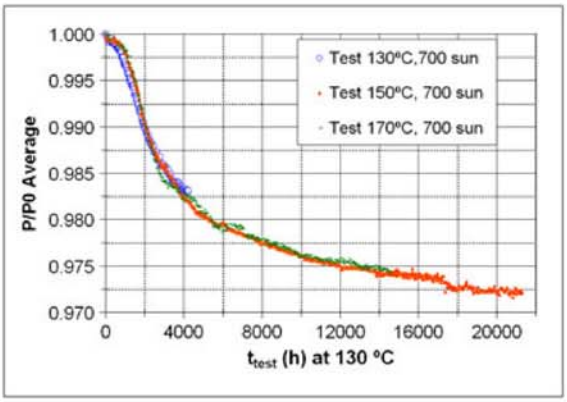

Figure 6. Measured average relative power curves at 700X. The times of the measured average relative power for the 150°C and 170°C curves were extrapolated based on T_{use} = 130°C.

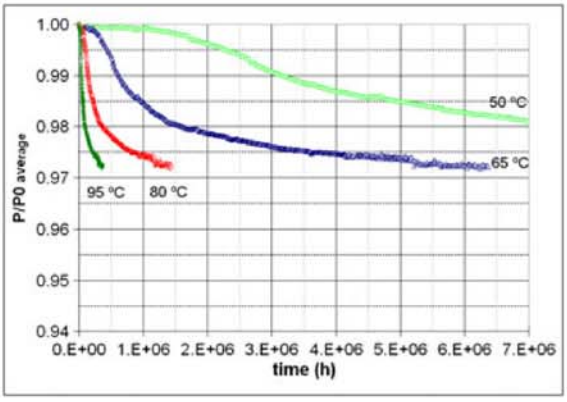

Figure 7. Relative average power evolution of the 700X cells as a function of operational temperature for continuous operation time.

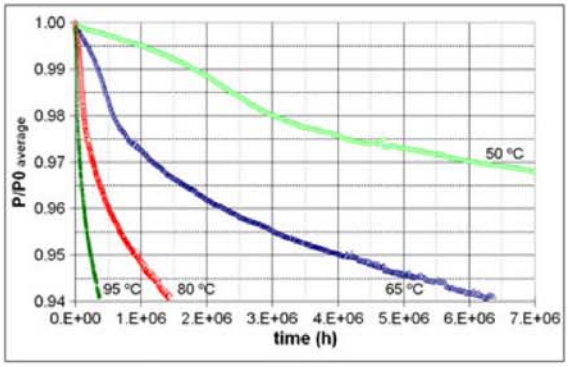

Figure 8. Relative average power evolution at 1050X as a function of the operational temperature for continuous operation time.

comparison of the effects of concentration on relative average power evolution. The following conclusions may be derived for all operational temperatures:

1. The evolution of the average relative power passed through three stages. Curves at 700X (Figure 7) presented an initial stage during which degradation was almost negligible, although this phase was not clearly observed for the 1050X cell (Figure 8). After the short initial stage, both concentrations exhibited an increase in the power degradation velocity until a third stage was reached, at which point the degradation trend stabilized.
2. During the second and third stages, the decreasing rate of the average relative power increased with concentration.
3. During the third stage at 700X, degradation tended to saturate, whereas at 1050X, the power degradation velocity decreased, but no degradation saturation was observed.
4. The ratio between the degradation rates (determined from the slope of each stage in the curves of the relative average power evolution in Figures 7 and 8) of the two concentrations exceeded 1.5 (the ratio of the concentrations) over the duration of the test. During the first stages, the ratio was high because degradation at 700X was negligible. During the second stage, the ratio was 1.7, and during the third stage it increased to 3.12.

In summary, both the power degradation velocity and the average relative power saturation associated with the degradation mechanism depended on the cell concentration. Larger concentrations resulted in larger corresponding values.

4. RELIABILITY AND WARRANTY ANALYSIS

It is important to distinguish measures of reliability and evaluation of warranty. Reliability is the probability that

a solar cell will operate for a given period of time without failure. The warranty time is associated with an agreement between the buyer and the seller (cell manufacturer), and is the time during which the seller promises to repair or replace any failed items. In this case, only replace the cell or receptor.

In this section, a reliability and warranty analysis is presented based on the degradation results described in Section 3. The solar cell degradation under operational conditions was evaluated assuming that the solar cells were operating under concentrated illumination for 8 h/day, followed by the absence of concentrated light during operating (0X condition test) for 16 h/day. To account for these two different operational conditions, t_{work} represents the accumulated time during which the solar cell was operating in the field.

As described earlier, no catastrophic failures were observed in any tests. Therefore, a reliability evaluation model based on the degradation data needed to be applied. The analysis described here relies on a model described elsewhere [17,20]. In these tests, we calculated the fraction of solar cells that degrade beyond a fixed failure power limit threshold (see Figure 9). This determination depends on the degradation data derived for each solar cell, (left graphs of Figure 4).

Figure 9 shows the model suitability for evaluating the reliability evolution during the life operational time (t_{work}). The normalized power probability density function for solar cells extrapolated to $T=65°C$ from the 150°C 700X curves (left Figure 4) is represented at different times. Two additional straight lines are plotted: a horizontal line corresponding to a power failure limit (FL) of 2.5% and a tilted line corresponding to the relative average power evolution at 700X for $T=65°C$. The slight asymmetry of the density power population indicated that a log-normal probability density function was required to fit the experimental data, as shown in Figure 9.

The probability density function at each time permits calculation of the fraction of cells above the failure power limit (which is, in fact, the reliability function, $R(t)$). Figure 10 shows the reliability function $R(t)$ for the 700X cell, obtained from Figure 9 for several FL values ranging from 1% to 10%.

The model used in Figure 9 to evaluate the reliability function R(t) at 700X, was applied to the corresponding solar cells at 1050X in Figure 11.

Figures 10 and 11 show a first stage during which $R(t) \approx 1$, a second stage during which $R(t)$ dropped abruptly (especially for low FL), and a third stage during which $R(t)$ dropped more slowly. The $R(t)$ slope depended on FL such that higher FL values produced lower $R(t)$ slopes. The initial period of stage two, characterized by a abruptly $R(t)$ drop, was the most interesting stage because it covered the range of $R(t)$ values that were suitable for warranty purposes.

A key reliability figure is MTTF, defined as the average period of time during which solar cells are expected to operate under nominal conditions before failure occurs. MTTF was evaluated by fitting $R(t)$ to a Weibull probability plot (WPP), and the Weibull parameters (β and η) were evaluated. For a prefixed FL, β parameter is roughly the same for the three test temperatures, according to a consistent failure degradation mechanism.

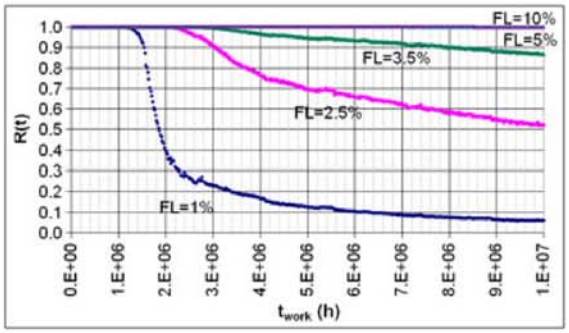

Figure 10. Reliability at 700X at an operational temperature of 65°C and for several failure limit values ranging from 1% to 10%.

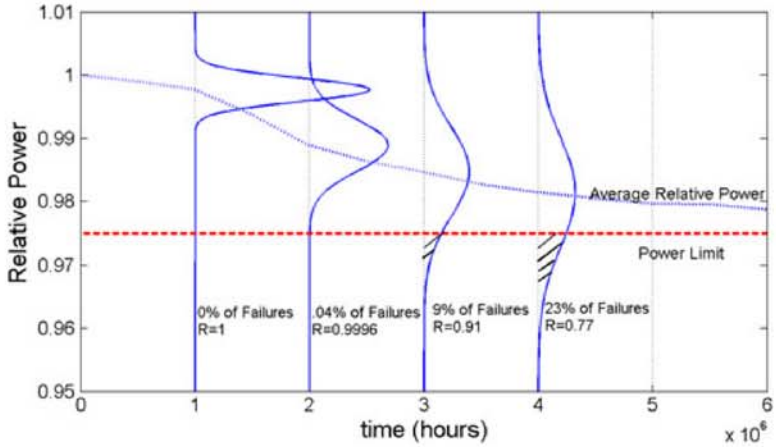

Figure 9. Time evolution of the average cell power probability density function at 700X. *R(t)* for four instants of t_{work} are also presented.

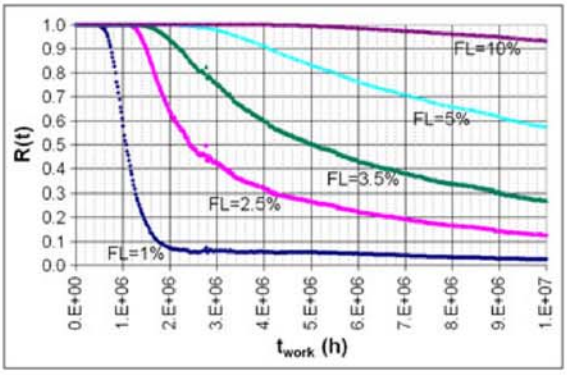

Figure 11. Reliability at 1050X for 65°C for several failure limit values ranging from 1% to 10%.

Weibull parameters permitted calculation of MTTF using Equation (3), [21]:

$$MTTF = \eta.\Gamma\left(1+\frac{1}{\beta}\right), \tag{3}$$

where Γ is the gamma function, η is the Weibull scale parameter, and β is the Weibull shape parameter. Table III shows the MTTF values calculated for the three possible operational temperatures and the two tested concentrations.

A more important parameter, from a practical perspective, is the warranty time, which is defined as the estimated time at which the reliability equals a specified probability of cells working without failure that suppose an adequate warranty costs. For example, if the manufacturer assumes the costs that 1% of the cell population fails within a warranty time (t_W), the time for which the warranty can be offered is the time at which the reliability is 0.99, that is, $t_{W(1\%)}$(y), in Table III. Warranty times were directly obtained from Figures 10 and 11. For example, the 700X cell operated at $T=65°C$ yielded a warranty time of 263 years (see Table III).

$$R\left(t_{W(1\%)}\right]_{FL=2.5\%,C=700X,T_{work}=65°C} = 263\text{y}\Big) = 0.99$$

Table III shows that the solar cell temperature and the concentration significantly affected the reliability during an assumed 30 years warranty period. More specifically,

- Solar cell temperature was the primary parameter, and concentration was the secondary determinant of warranty time.
- For a $T=65°C$ operational temperature, a 30-year warranty may be offered for both concentration cells (700X and 1050X) with a lower cell population fails of 0.1%.
- For a $T=95°C$ operational temperature, a 30-year warranty may not be offered for either concentration cell (700X or 1050X) for any limit of cell population fails from 0.1% to 10%.
- For a $95°C > T > 65°C$, the possibilities for offering a 30-year warranty depend on the cell concentration, and the cost limit of cell population fails that the seller promises to replace.

Solar cell temperature was the primary determinant of reliability and warranty time.

The temperature difference between the sets of solar cells emulated at each concentration (700X and 1050X) was only 2°C [13] because the solar cell circuit boards used in these tests were prepared using good thermal designs. Forever, the emulated concentration is basically the only difference between the two set of solar cells.

Solar cell concentration was the secondary determinant of reliability and warranty time

The small solar cells (1 mm^2) used in this work (which were designed and manufactured according to a LED-like approach [22]), together with an appropriate thermal design (65°C in working conditions), could easily be offered with a 30−year warranty at an $FL=2.5\%$ for operation at a concentration of at least 1050X.

5. VALIDITY RANGE OF PREDICTIONS

As CPV installations based on III–V solar cells are relatively new, there is not a need for long-time experience in field in order to identify the combination of accelerated stress tests that duplicate field failure. Accordingly, this work presents the reliability predictions from temperature accelerated aging tests in concentrator solar cells as a first contribution to which should be the combination of tests

Table III. Mean time to failure values for several operational conditions and assuming $FL=2.5\%$, in agreement with Section 3. A cell working time of 8 h/day was assumed. Warranty times in years [$t_{W(\%)}$(y)] for several cell population fails (0.1–10%).

	$T=65°C$		$T=80°C$		$T=95°C$	
Concentration	700	1050	700	1050	700	1050
MTTF (10^6 h)/(years)	25.0/2854	4.08/466.4	5.64/644.6	0.92/105.3	1.43/164.3	0.23/26.8
$t_{W(0.1\%)}$(years)	235	127.5	53.1	28.8	13.5	7.3
$t_{W(1\%)}$ (years)	263	142.1	59.4	32.1	15.1	8.2
$t_{W(5\%)}$ (years)	310	157.5	70.0	35.6	17.9	9.1
$t_{W(10\%)}$(years)	347	170.7	78.5	38.5	20.0	9.8

that will emulate and accelerate field conditions. Therefore, subsequent works presenting aging tests based on illumination, humidity, and others are required.

Additionally, our predictions on the basis of temperature stress have a limited validity. For example, we are not absolutely sure if the failure mechanism that appears in our tests will be the same as that in real operation, although previous experiments for 1-year real operation [20] with this type of cells shows that they suffer a very low degradation without any catastrophic failures. This is consistent with our experiments, but it is necessary to confirm that the degradation mechanism for long time operation in field is the same in order to apply the numerical reliability and warranty results obtained in these tests. Also, it is necessary to take into account that each commercial encapsulation approach could exhibit specific weakness. For example, a given cell encapsulation could not resist a temperature of 170°C such as the one used in our tests.

Finally, the results of this work cannot be directly applied to current commercial triple junction solar cells mainly because they are grown on germanium substrates what could produce different failure mechanisms.

6. SUMMARY AND CONCLUSIONS

Accelerated aging tests of single junction GaAs concentrator solar cells were conducted at three temperatures (130°C, 150°C, and 170°C) and emulated concentration ratios (0X, 700X, and 1050X). The accumulated duration of the tests exceeded 10 000 h. The main conclusions of the tests are as follows: No catastrophic failure was observed, although gradual relative power degradation occurred in all tests and was responsible for failure. The evolution of the relative power of the solar cells tested was assessed to obtain an average power and dispersion for all conditions tested. The activation energy was calculated for the mechanism responsible for degradation and failure. The calculated activation energy was 1.02 ± 0.04 eV. This is the first time this activation energy has been calculated for III–V terrestrial concentrator solar cells, and this value was used to extrapolate the evolution of the relative power at any temperature of solar cell operation. The solar cells power evolution was used to obtain the reliability at different operational temperature of cell. The conclusions of the reliability analysis are the following: A 2.5% solar cell power loss was defined as the failure limit *(FL)*. At this limit, the other elements of the CPV system contributed to the remaining power loss up to a 20% failure limit for the system. A value of 2.5% is considered to be conservative.

The failure limit definition permitted evaluation of the reliability function, $R(t)$, MTTF, and warranty times. For an operational temperature of $T = 65$°C (expected operation temperature of solar cells), a 30-year warranty may be offered for both concentration cells. For an operational temperature of $T = 95$°C, a 30-year warranty cannot be offered for either concentration cell (700X and 1050X) at any proportion of population cells that fails (from 0.1% to 10%). For operational temperatures of $95°C > T > 65°C$, the option to offer a 30-year warranty depends on the cost limit that the seller assumes.

Therefore, solar cell temperature was the primary determinant, and concentration was the secondary determinant of reliability and warranty time.

The next objective is to evaluate the reliability of MJSCs, for which a new test setup is being developed.

Small solar cells, such as the 1 mm^2-size cells used in this work, manufactured using an appropriate thermal design, may easily be offered with a 30-year warranty for a failure limit of 2.5% power loss under the operational conditions of a concentration of at least 1050X.

ACKNOWLEDGEMENTS

This work was supported by the European Commission under the project NGCPV A new generation of concentrator photovoltaic solar cells, modules and systems' with Grant agreement no. 283798 and by the Spanish Ministerio de Educación y Ciencia with the CONSOLIDER-INGENIO 2010 program by means of the GENESIS FV project (CSD2006-004). The Spanish Ministerio de Ciencia e Innovación also contributed with the INNPACTO program by means of the SIGMAMODULOS IPT-2011-1441-920000 project (PSS-440000-2009-30), project reference TEC2008-01226. This project was supported from the Comunidad de Madrid under the NUMANCIA II program (S2009/ENE1477).

REFERENCES

1. Algora C, Rey-Stolle I, García I, Galiana B, Espinet P, Baudrit M, Barrigon E. A dual junction solar cell with an efficiency of 32.6% at 1000 suns and 31.0% at 3000 suns. *5th Intern. Conf. for the Generation of Electricity*, Nov. 2008.
2. Green MA, *et. al*. Solar cell efficiency tables (version 39). *Prog. Photovolt: Res. Appl.* 2012; **20**: 12–20. DOI: 10.1002/pip.2163
3. Araki K, et al. Development of concentrator modules with dome-shaped Fresnel lenses and triple-junction concentrator cells. *Progress in Photovoltaics: Res Appl* 2005; **13**: 513–527. DOI: 10.1002/pip.643
4. IEC 62108 Ed 1.0: concentrator photovoltaic (CPV) modules and assemblies—design qualification and type approval. 2007.
5. Algora C. Reliability of III–V concentrator solar cells. *Microelectronics Reliability* 2010; **50**: 1193–1198.
6. Rubio F, Martínez M, Hipólito A, Martín A, Banda P. Status of CPV technology. *25th European Photovoltaic Solar Energy Conference and Exhibition (25th EU PVSEC)*. Valencia, Spain. 2010, DOI: 10.4229/25thEUPVSEC2010-1DV.5.46

7. Vázquez M, Algora C, Rey-Stolle I, González JR. III–V concentrator solar cell reliability prediction based on quantitative LED reliability data. *Progress in Photovoltaics: Res Appl* 2007; **15**(6). DOI: 10.1002/pip.753.
8. González JR, Vázquez M, Núñez N, Algora C, Rey-Stolle I, Galiana B. Reliability analysis of temperature step-stress tests on III-V high concentrator solar cells. *Microelectronics Reliability* 2009; **49**: 673–680. DOI: 10.1016/j.microrel.2009.04.001
9. Arrhenius S. *Zeitschrift für Physikali sche Chemie* 4, 226- (1889)4, 226 _(1889)_, translated into English in *Selected Readings in Chemical Kinetics*, Back MH, Laidler KJ (eds). Oxford: Pergamon, NY, 1967.
10. Escobar LA, Meeker WQ. A review of accelerated test models *Statistical Science* 2006; **21**: 552–577. DOI: 10.1214/088342306000000321
11. Núñez N, Vázquez M, González JR, Algora C, Espinet P. Novel accelerated testing method for III–V concentrator solar cells *Microelectronics Reliability* 2010; **50**: 1880–1883. DOI: 10.1016/j.microrel.2010.07.085
12. Yang G. *Life Cycle Reliability Engineering*. Chapter 7. John Wiley & Sons, Inc: Hoovoken, New Jersey, 2007.
13. Núñez N, Vázquez M, González JR, Jiménez FJ, Bautista J. Instrumentation for accelerated life tests of concentrator solar cells. *The Review of Scientific Instruments* 2011; **82**: 024703. DOI: 10.1063/1.3541800
14. Antón I, Sala G, Heasman K, Kern R, Bruton TM. Performance prediction of concentrator solar cells and modules from dark I–V characteristics. *Prog Photovolt: Res Appl.* 2003; **11**: 165–78. DOI: 10.1002/pip.477
15. Algora C, Rey-Stolle I, Galiana B, González JR, Baudrit M, García I, et al. III–V concentrator solar cells as LEDs. In *Proceedings of the 20th European Photovoltaic Solar Energy Conference*, 2005; 82–5. DOI: 10.1016/S0961-1290(05)71233-3
16. Galiana B, Algora C, Rey-Stolle I. Comparison of 1D and 3D analysis of the front contact influence on GaAs concentrator solar cell performance. *Solar Energy Materials & Solar Cells* 2006; **90**(16): 2589–2604. DOI: 10.1016/j.solmat.2006.02.013
17. Vázquez M, Rey-Stolle I. Photovoltaic module reliability model based on field degradation studies. *Prog Photovolt: Res Appl* 2008; **16**: 419–433. DOI: 10.1002/pip.825
18. *Design for Reliability*, Crowe D, Feinberg A (eds). CRC Press: Boca Raton London New York Washington, D.C, 2001.
19. Algora C. Very high concentration challenges of III–V multijunction solar cells. In Chapter 5 of the book *Concentrator Photovoltaics*, Luque A, Andreev V (eds). Springer: Heidelberg, Germany, 2007. ISBN 978-3-540-68796-2
20. González JR, Vázquez M, Algora C, Núñez N. Real-time reliability test for a CPV module based on a power degradation model. *Prog Photovolt: Res Appl* 2011; **19**: 113–122, 2011. DOI: 10.1002/pip.991
21. Cohen AC. Maximum likelihood estimation in Weibull distribution based on complete and censored samples. *Technometrics* 1965; **7**; 579–588. DOI: 10.1093/hmg/ddq003
22. Algora C, et al. Strategic options for a LED-like approach in III–V concentrator photovoltaics. In *Proceedings of the 2006 IEEE 4th World Conference Photov. Energy Conv*, Hawaii (USA), 2006; 741–744. ISBN: 1-4244-0016-3